NANOSYSTEMS:
PHYSICS, CHEMISTRY, MATHEMATICS

Popov A. L., et al. *Nanosystems: Phys. Chem. Math.*, 2022, **13** (2), 204–211.
http://nanojournal.ifmo.ru
DOI 10.17586/2220-8054-2022-13-2-204-211

Original article

Synthesis and analysis of cerium-containing carbon quantum dots for bioimaging *in vitro*

A. L. Popov[1,a], I. V. Savintseva[1,b], A. M. Ermakov[1,c], N. R. Popova[1,d], D. D. Kolmanovich[1,e], N. N. Chukavin[1,2,f], A. F. Stolyarov[1,g], A. B. Shcherbakov[3,h], O. S. Ivanova[4,j], V. K. Ivanov[4,k]

[1]Institute of Theoretical and Experimental Biophysics of the Russian Academy of Sciences, 142290, Russia
[2]Moscow Region State University, 141014, Moscow, Russia
[3]Zabolotny Institute of Microbiology and Virology, National Academy of Sciences of Ukraine, Kyiv D0368, Ukraine
[4]Kurnakov Institute of General and Inorganic Chemistry of the Russian Academy of Sciences, Moscow, 119991, Russia

[a]antonpopovleonid@gmail.com, [b]savintseva_irina@mail.ru, [c]ao_ermakovy@rambler.ru,
[d]nellipopovaran@gmail.com, [e]kdd100996@mail.ru, [f]chukavinnik@gmail.com,
[g]a.f.stolyaroff@gmail.com, [h]ceroform@gmail.com, [j]runetta05@mail.ru, [k]van@igic.ras.ru

Corresponding author: A. L. Popov, antonpopovleonid@gmail.com

PACS 68.65.-k, 81.20.-n, 82.70. Dd, 87.80.-y

ABSTRACT The latest biomedical approaches based on the use of nanomaterials possessing luminescent properties make it possible to effectively visualize cancer cells or tissues, thus expanding diagnostic capabilities of the current bioimaging techniques. In this paper, a new scheme is proposed for the synthesis of cerium-containing carbon quantum dots (Ce-Qdots) of ultra-small size, promising for biomaging. Ce-Qdots have a high degree of biocompatibility, as well as remarkable redox activity. Cytotoxicity analysis performed using 4 human cell cultures confirmed the high degree of Ce-Qdots biocompatibility. It was shown that Ce-Qdots in concentrations up to 200 μg/ml do not have a negative effect on the metabolic, proliferative, migration and clonogenic activity of cell cultures after 24, 48 and 72 hours of co-incubation. Ce-Qdots can be considered as the basis of a new theranostic agent for bioimaging and targeted delivery of biologically active substances.

KEYWORDS carbon dots, quantum dots, ceria, bioimaging, cell uptake, viability, luminescence.

ACKNOWLEDGEMENTS The work was supported by the Russian Science Foundation (project 20-74-00086).

FOR CITATION Popov A.L., Savintseva I.V., Ermakov A.M., Popova N.R., Kolmanovich D.D., Chukavin N.N., Stolyarov A.F., Shcherbakov A.B., Ivanova O.S., Ivanov V.K. Synthesis and analysis of cerium-containing carbon quantum dots for bioimaging *in vitro*. *Nanosystems: Phys. Chem. Math.*, 2022, **13** (2), 204–211.

1. Introduction

Bioimaging is one of the most promising and actively developing tools for socially significant diseases diagnosis. The development of this technology is associated with a significant breakthrough in the design and functionalization of carbon quantum dots (Qdots), which characteristics can be tuned at the synthesis stage and additionally modified with chemical agents in order to impart the necessary biological activity [1–3]. Carbon quantum dots possess unique luminescent characteristics: multi-color emission, customizable optical properties, high quantum yield, excellent photostability and solubility in water, as well as good biocompatibility, which allows them to be used in various biomedical applications [4, 5]. It is also worth noting that carbon quantum dots can be synthesized through simple schemes and methods, such as hydrothermal or microwave, using inexpensive chemical reagents [6, 7].

Today, methods are being developed for obtaining carbon quantum dots for selective visualization of various types of cells (cancer, stem or neuronal) with the possibility of tracking them *in vivo*, providing selective accumulation in given cell types [8]. There are also techniques for obtaining functionalized quantum dots for precise visualization of individual cell organoids [9]. Quantum dots are widely used for early cancer diagnosis by functionalizing their surface with cancer cell-specific molecules or antibodies. For example, an effective accumulation was shown of PEG-labeled quantum dots modified with the peptide angiopep-2, which provided selective accumulation in human glioblastoma cells and effectively visualized the tumor [10]. Earlier, pH-sensitive carbon quantum dots were synthesized for HeLa cells visualization [11]. Thus, the design of carbon quantum dots capable of not only effectively visualising tumor cells, but also providing a therapeutic effect, is a frontier area of nanomedicine.

One of the most promising agents for nanomedicine, which has pronounced therapeutic activity and the ability to provide a synergistic effect with the other medicinal substances, is cerium oxide. We have previously shown that a nanocomposite based on cerium oxide and curcumin is capable of protecting normal cells under H_2O_2-induced oxidative stress, and inhibit metabolic activity of tumour cells in a time-increasing manner [12]. We also demonstrated the synergistic effect of cerium oxide nanoparticles with tumor necrosis factor, increasing cytotoxicity for A-549 and HEp-2 cancer cells [13]. The functionalization of cerium oxide nanoparticles with D-panthenol provides an increased antioxidant and UV-protective effect better than individually panthenol or CeO_2 nanoparticles [14].

Here, we proposed a new synthesis scheme of organic carbon quantum dots, modified with cerium for additional biological activity, and carried out a comprehensive analysis of their cytotoxicity using cancer and normal cells.

2. Materials and methods

2.1. Synthesis and characterization of Ce-Qdots

Ce-Qdots were synthesized by the hydrothermal method using a teflon autoclave. At the first stage, 0.8 g of $Ce(NO_3)\cdot 6H_2O$, 1 g of citric acid and 1 g of carbamide were dissolved in 20 ml of deionized water on a magnetic stirrer. After dissolution, 1.1 ml of polyethylenepolyamine (PEPA) was added and stirring was continued for 20 minutes at a temperature of 25°C. Next, the resulting suspension was transferred to an autoclave and heated at a temperature of 240°C for 4 hours. After cooling to room temperature, the resulting Q-dots colloid solution was separated from the precipitate by centrifugation at 3000 rpm and further purified by dialysis (1 kDa bag) for 48 hours against distilled water. The resulting solution was dried at 50°C.

2.2. Cell cultures

We used 4 types of cell cultures from Cell&Tissue biobank of the Institute of Theoretical and Experimental Biophysics of the Russian Academy of Sciences: MNNG/Hos human osteosarcoma, NCI-ADR human ovarian adenocarcinoma, MCF-7 human breast adenocarcinoma and human mesenchymal stem cells (MSCc) isolated from dental pulp. Cells were cultured in DMEM/F12 medium containing with 10% fetal calf serum and 200 units of penicillin/streptomycin at 37°C under 5% CO_2 atmosphere. Cells were removed from culture flasks using 0.25% trypsin-EDTA solution after washing them three times with Hanks' buffer.

2.3. MTT assay

Analysis of cell viability after 24 or 72 hours incubation with Ce-Qdots was performed using the MTT assay. Cells were seeded in 96 well plates at a density of $2.5\cdot 10^4/cm^2$ in a DMEM/F12 culture medium containing 10% fetal calf serum. After 8 hours, Ce-Qdots (1-200 μg/ml) were added by changing the culture medium. Then, after 24 and 72 hours, the medium was replaced with a medium with a solution of the MTT reagent (0.5 mg/mL) and further analysis was carried out according to the standard method [15].

2.4. Fluorescent microscopy

Intracellular visualization using Ce-Qdots was performed using an inverted fluorescence microscope Zeiss Axiovert 200. Cells were seeded in 35 mm Petri dishes with a central hole (Ibidi, Germany) at a density of $2.5\cdot 10^4/cm^2$ in a DMEM/F12 culture medium containing 10% fetal calf serum. Afterwards, Ce-Qdots were added to the cells at a concentration of 100 μg/mL. After 24 hours, microphotography of cell cultures was carried out after washing three times with a Hanks buffer. The luminescence of CeO_2-Qdots localized on the cell surface was inhibited by treating the cells with trypan blue.

2.5. Clonogenic assay

Clonogenic analysis was performed after 24 hours of incubation with Ce-Qdots. Cells were seeded in 6 well plates (SPL, Korea) at a density of $1.5\cdot 10^3$ cells per well. After 8-11 days (depending on the type of cell culture), the formed colonies were fixed using 4% paraformaldehyde and stained with 0.1% methylene blue solution. Cell aggregates containing more than 50 units were considered as a formed colony.

2.6. Migration assay

Analysis of cell migration after incubation with Ce-Qdots was performed within 48 hours after artificial scratch formation. 2-well silicone inserts (Ibidi, Germamy) were used to form the scratch. The cells were seeded in the inserts at a density of $2.5\cdot 10^4$ cm^{-2} after the formation of a monolayer. Further, various concentrations of Ce-Qdots (50, 100, and 200 μg/mL) were added to the cells for 3 hours, and then the insert was removed. The process of healing of the model wound was monitored by microphotography for 48 hours every 6 hours.

2.7. Statistical analysis

Data are presented as standard deviation from the mean value. The significance of differences between experimental groups was assessed by the Mann-Whitney U-test.

3. Results

The synthesis of Ce-Qdots was carried out according to the scheme shown in Fig. 1a. According to TEM data, the particle size of the Ce-Qdots was 2–3 nm (Fig. 1b). According to UV–visible spectroscopy the position of the absorption peak of the Ce-Qdots was at 390 nm. The peak of the emission of the Ce-Qdots was at 450 nm (Fig. 1c). The hydrodynamic radius of the Ce-Qdots upon dilution in water was about 40–50 nm (Fig. 1d). Zeta potential of the particles when diluted in distilled water was -32 ± 1.1 mV. The synthesized Ce-Qdots demonstrated good colloidal stability and can be stored for at least 90 days without any signs of precipitation.

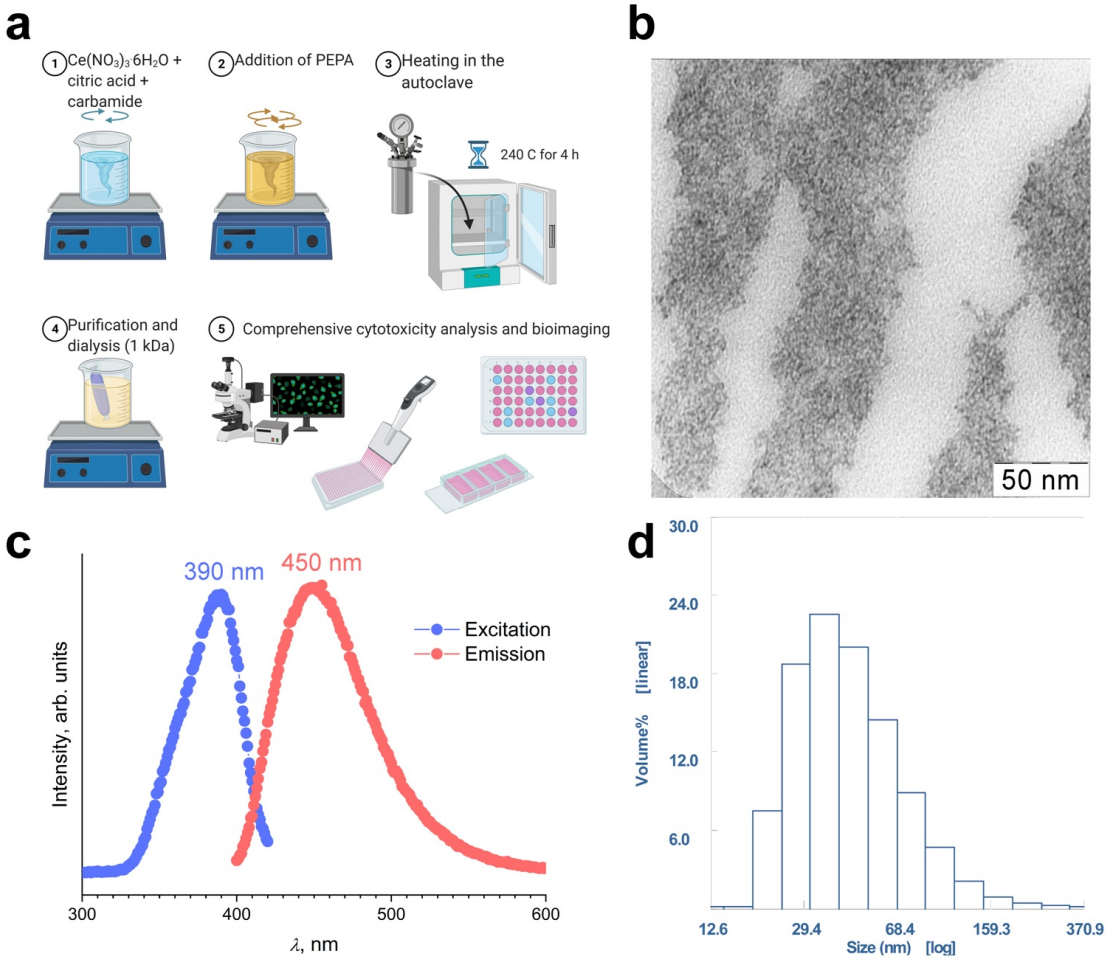

FIG. 1. Synthesis scheme of the Ce-Qdots (a), transmission electron microscopy (b), emission and excitation spectra(c), dynamic light scattering in MQ water (d)

The MTT assay was used to study the metabolic activity of cell cultures after 24, 48 and 72 hours incubation with Ce-Qdots (Fig. 2). It was shown that Ce-Qdots do not affect the metabolic activity of human MSCs at concentrations up to 200 μg/mL, which confirms a high level of biocompatibility (Fig. 2a). It is well known that human MSCs are a rather sensitive culture and can react to toxic agents by spontaneous differentiation or by stopping proliferation [16]. It was previously shown that carbon dots obtained by pyrolysis of a hydrazine solution have a high quantum yield and do not exhibit cytotoxicity against human neuronal MSCs in concentrations up to 100 mg/mL, and are also very effective for their visualization [17]. Citric acid-based carbon dots did not have a toxic effect on rat bone marrow mesenchymal stem cells in concentrations below 50 μg/mL, did not affect their subsequent ability to differentiate and were visualized easily [18]. Ce-Qdots did not cause a decrease in metabolic activity (1–200 μg/mL) after 24 and 48 hours incubation of human osteosarcoma MNNG/Hos cell cultures and radioresistant ovarian carcinoma cells NCI/ADR (Fig. 2c,d). Meanwhile, after 72 hours of incubation, there was a significant decrease in the viability level of MNNG/Hos cells at a Ce-Qdots concentration of 20 μg/mL, and also a decrease in the viability level of NCI/ADR cells at a Ce-Qdots concentration of 50 μg/ml. Human adenocarcinoma cell culture MCF-7 did not decrease its viability level after 72 hours of incubation with Ce-Qdots in the whole concentration range (1–200 μg/mL) (Fig. 2b).

The appearance of the cell cultures after 24 hours of incubation with Ce-Qdots in a wide range of concentrations (1–200 μg/mL) is shown in Fig. 3. Micrographs confirm that synthesized Ce-Qdots, even at the highest concentrations

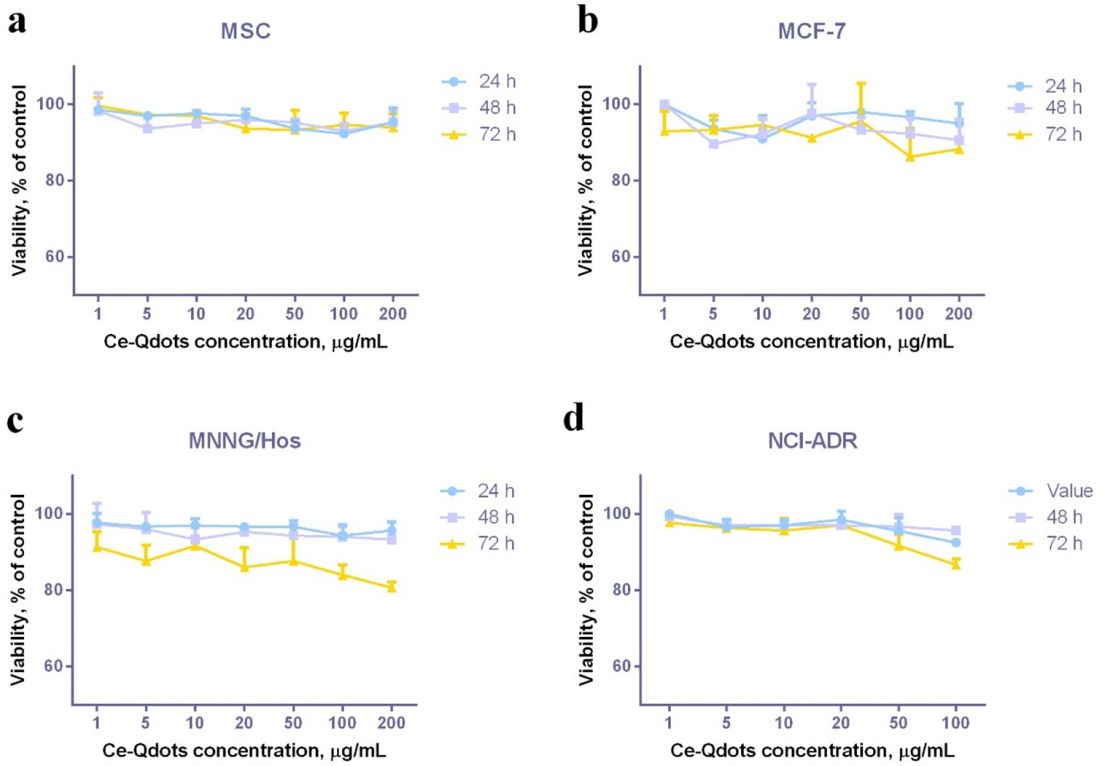

FIG. 2. Cytotoxicity analysis of Ce-Qdots (1–200 μg/mL) by the MTT assay using human MSC, MNNG/Hos, MCF-7 and NCI/ADR cell lines (24, 48 and 72 hours after incubation)

(100 and 200 μg/mL), do not have a negative effect on MSC, MNNG/Hos, MCF-7 and NCI/ADR cell lines cells. Morphological and phenotypic characteristics of cell cultures also do not change.

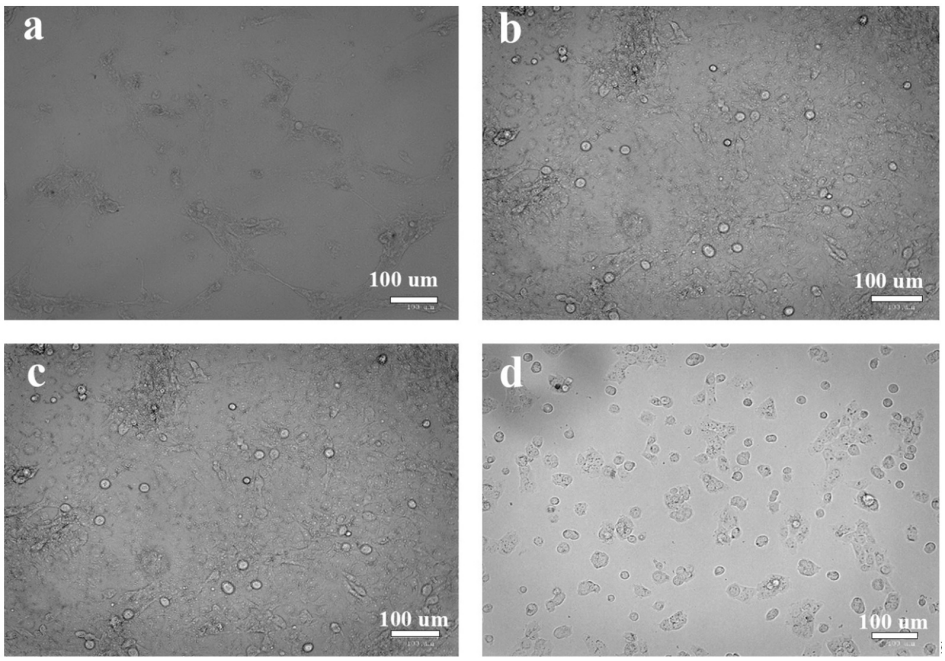

FIG. 3. The appearance of MSC (a), MNNG/Hos (b), MCF-7 (c), NCI/ADR (d) cell cultures after 16 hours incubation with Ce-Qdots (100 μg/mL)

Next, the clonogenic activity of cell cultures was evaluated after incubation with Ce- Qdots at a maximum concentration of 200 μg/mL. Cellular cooperation is one of the most important fundamental factors for their proliferation [19]. The action of paracrine factors stimulate the proliferative activity of neighboring cells, determining the rate of colony

formation [20]. We have shown the absence of the effect of Ce-Qdots on the clonogenic activity of 3 types of cell cultures - MCF-7, human MSCs NCI/ADR (Fig. 4). The MNNG/Hos human osteosarcoma cell culture showed a significant decrease in the number of formed colonies (up to 30% compared to the control), which confirms the MTT assay data. In a similar way, we have previously shown that cerium oxide nanoparticles can exhibit selective cytotoxic activity against certain types of cancer cells [21].

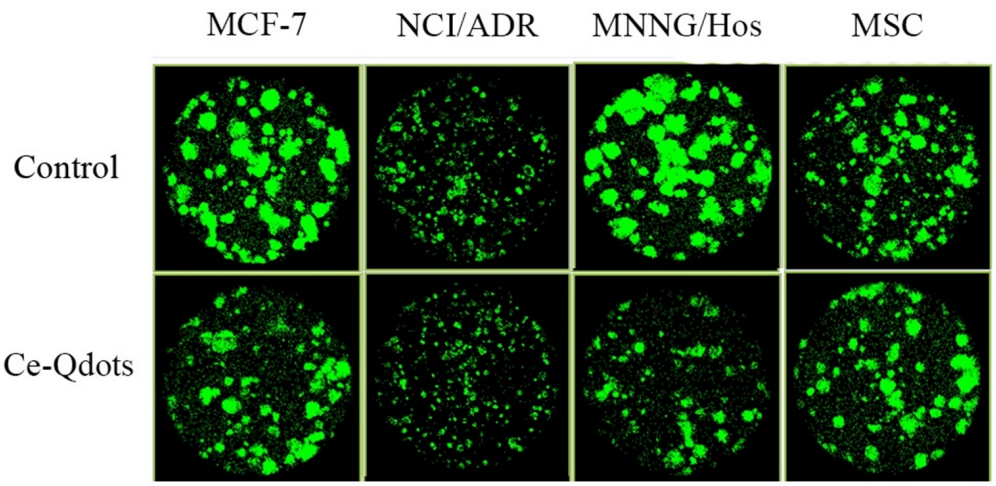

FIG. 4. Clonogenic analysis of Ce-Qdots (200 μg/mL) using human MSC, MNNG/Hos, MCF-7 and NCI/ADR cell lines (24 hours after incubation, cultivation for 264 hours)

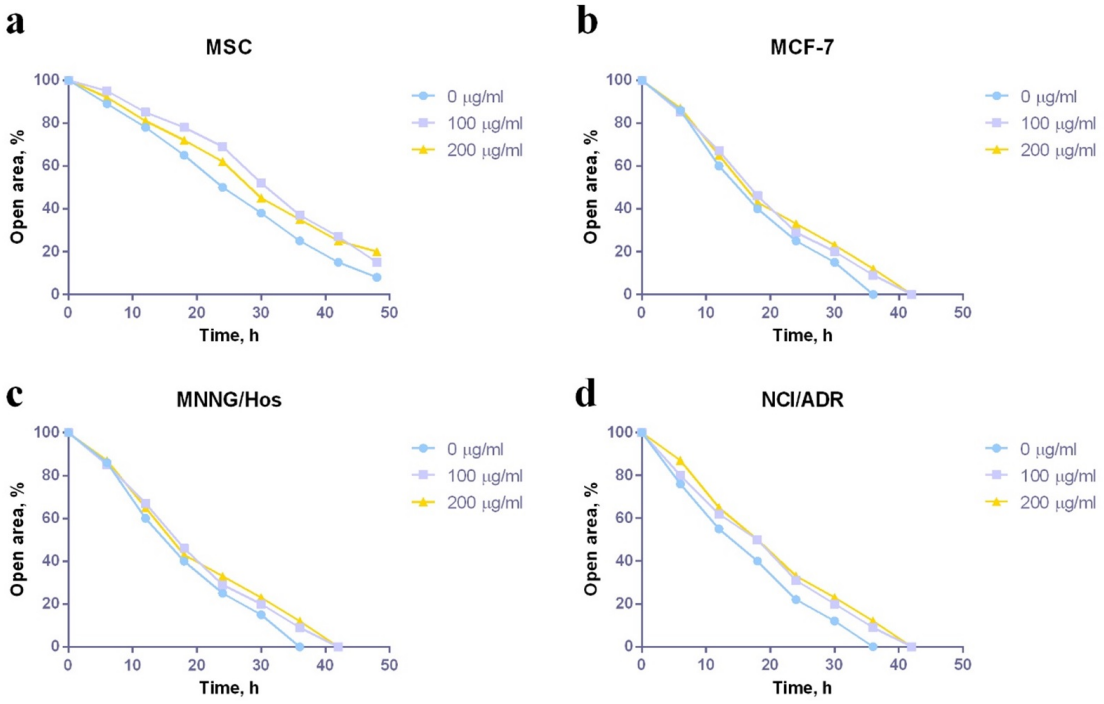

FIG. 5. Migration assay of Ce-Qdots (100 and 200 μg/mL) using human MSC, MNNG/Hos, MCF-7 and NCI/ADR cell lines (24 hours after incubation, cultivation for 48 hours). The analysis was carried out by assessing the open area of the model wound every 6 hours using a Clone Select Imager plate reader

Analysis of migration activity of cell cultures after incubation with carbon dots was performed by means of scratch test. The analysis of migration activity showed the absence of toxicity of Ce-Qdots for all studied concentrations (100 and 200 μg/mL) (Fig. 5). The migration activity of cells is one of the key indicators of the metabolic activity of cells [22]. Importantly, the migration activity of cells is associated not only with the metabolic activity of cells, but also with the efficiency of endocytosis of the nanoparticles [23]. For example, it was previously shown that ultra-small cerium oxide

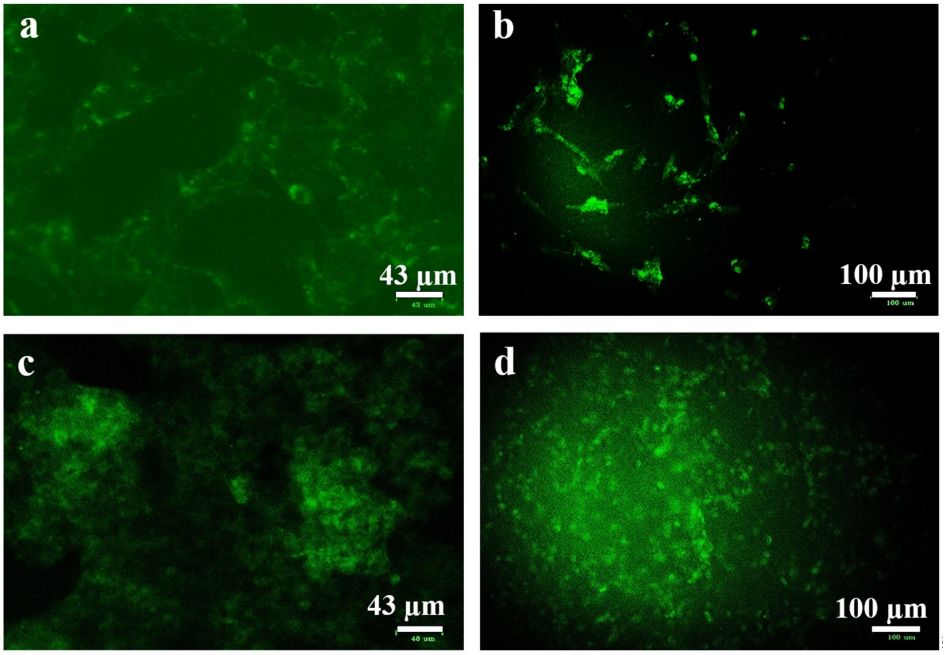

FIG. 6. Fluorescent inverted microscopy images of human MSC (a), MNNG/Hos (b), MCF-7 (c) and NCI/ADR cell lines labeled with 100 μg/ml Ce-Qdots (100 μg/mL). Before the analysis, the cells were washed three times with a phosphate buffer

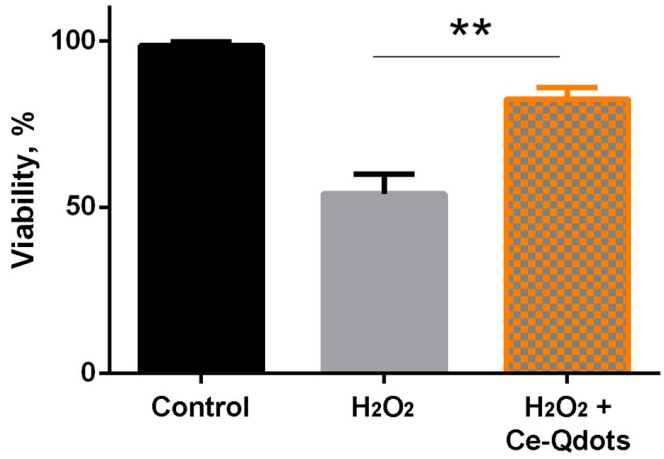

FIG. 7. Protective effect of Ce-Qdots (100 μg/ml) on MSCs under oxidative stress conditions induced by H_2O_2 treatment (as assessed using MTT assay). The cells were pretreated with Ce-Qdots (100 μg/ml) and then treated with hydrogen peroxide (500 μM for 30 min). Data are presented at mean $\pm$ SD, * p$\leq$0.05%, ** p$\leq$0.001%

nanoparticles (3 nm) inhibit the migration and proliferation of gastric cancer by increasing DHX15 expression [24]. Chen et al. demonstrated that pristine carbon quantum dots/Cu_2O composite selectively inhibited ovarian cancer SKOV3 cells ($IC_{50} = 0.85$ μg/mL) by targeting cellular microenvironment, such as matrix metalloproteinases, angiogenic cytokines and cytoskeleton. In addition, CQDs/Cu_2O has a notable effect on transcriptional regulation of multiple genes in SKOV3 cells, where 495 genes were up-regulated and 756 genes were down-regulated [25].

The analysis of intracellular fluorescence of Ce-Qdots (100 μg/mL) showed their effective endocytosis into various cells (Fig. 4). The ultra-small size of nanoparticles allows for their effective penetration into the cytoplasm of cells [26]. The highest efficiency of uptake was typical of adenocarcinoma cells of the MCF-7 line and MNNG/Hos osteosarcoma cells (Fig. 4c,b). Mesenchymal stem cells also actively uptook Ce-Qdots, but less effectively than cancer cells (Fig. 4a). Such a difference in Ce-Qdots uptake efficiency may be associated not only with different metabolic activity of cells, but also with the efficiency of endocytosis, which is always higher in cancer cells than in primary cell culture like human MSC. Radioresistant NCI/ADR cells were also loaded with Ce-Qdots dots with high efficiency.

To confirm Ce-Qdots bioactivity, especially their antioxidant properties, we analyzed their protective activity in a H_2O_2-induced oxidative stress model. It was shown that a 30 minute exposure to hydrogen peroxide leads to a decrease in the viability of MSCs up to 57%. Pretreatment of the cell culture with carbon dots at a concentration of 100 μg/ml provided a pronounced protective effect, which was expressed in maintaining a high level of viability of the cell culture upon exposure to an oxidizer (Fig. 7). Hydrogen peroxide actively penetrates into the cell, causing lipid peroxidation, oxidation and crosslinking of proteins, DNA strand breaks, which generally leads to intracellular oxidative stress and ultimately to apoptosis [27]. It was previously shown that cerium dioxide nanoparticles effectively protect cells from hydrogen peroxide action [28]. It was also shown that various types of cells, including myoblasts, nerve cells, fibroblasts, can be effectively protected from the action of exogenous hydrogen peroxide by cerium-containing compounds including CeO_2 nanoparticles [29, 30]. It is worth noting that the catalase-like activity of cerium oxide nanoparticles is pH dependent, which is very promising for tumor therapy [31]. The same pH dependence could be anticipated for Ce-Qdots, too.

4. Conclusions

A two-stage scheme of synthesis of cerium-containing carbon dots is proposed. This scheme is very convenient, it involves the use of inexpensive reagents, that makes it possible to obtain the carbon capable of being effectively internalized by various types of cells. Obtained Ce-Qdots have high biocompatibility and antioxidant activity, providing good protection of living cells from oxidative stress.

References

[1] Liu Q., Guo B.D., Rao Z.Y., Zhang B.H., Gong J.R. Strong two-photon-induced fluorescence from photostable, biocompatible nitrogen-doped graphene quantum dots for cellular and deep-tissue imaging. *Nano Lett.*, 2013, **13**, P. 2436–2441.

[2] Ruan S.B., Qian J., Shen S., Zhu J.H., Jiang X.G., He Q., Gao H.L. A simple one-step method to prepare fluorescent carbon dots and their potential application in non-invasive glioma imaging. *Nanoscale*, 2014, **6**, P. 10040–10047.

[3] Zholobak N.M., Popov A.L., Shcherbakov A.B., Popova N.R., Guzyk M.M., Antonovich V.P., Yegorova A.V., Scrypynets,Y.V. Leonenko I.I., Baranchikov A.Ye., Ivanov V.K. Facile fabrication of luminescent organic dots by thermolysis of citric acid in urea melt, and their use for cell staining and polyelectrolyte microcapsule labelling. *Beilstein Journal of Nanotechnology*, 2016, **7**, P. 1905–1917.

[4] Zhang J., Yu S.H. Carbon dots: large-scale synthesis, sensing and bioimaging. *Mater. Today*, 2016, **19**, P. 382–393.

[5] Xu Q., Li B., Ye Y., Cai W., Li W., Yang C., Chen Y., Xu M., Li N., Zheng X., Street J., Luo Y., Cai L. Synthesis, mechanical investigation, and application of nitrogen and phosphorus co-doped carbon dots with a high photoluminescent quantum yield. *Nano Res.*, 2018, **11**, P. 3691–3701.

[6] Hamd-Ghadareh S., Salimi A., Fathi F., Bahrami S. An amplified comparative fluorescence resonance energy transfer immunosensing of CA125 tumor marker and ovarian cancer cells using green and economic carbon dots for bio-applications in labeling, imaging and sensing. *Biosensors and Bioelectronics*, 2017, **96**, P. 308–316.

[7] Roy P., Chen P.C., Periasamy A.P., Chen Y.N., Chang H.T. Photoluminescent carbon nanodots: synthesis, physicochemical properties and analytical applications. *Mater. Today*, 2015, **18**(8), P. 447–458.

[8] Zheng X.T., Ananthanarayanan A., Luo K.Q., Chen P. Glowing graphene quantum dots and carbon dots: properties, syntheses, and biological applications. *Small*, 2015, **11**(14), P. 1620–1636.

[9] Shang W., Zhang X., Zhang M., Fan Z., Sun Y., Han M., Fan L. The uptake mechanism and biocompatibility of graphene quantum dots with human neural stem cell. *Nanoscale*, 2014, **6**, P. 5799–5806.

[10] Mo L., Li J., Liu Q., Qiu L., Tan W. Nucleic acid-functionalized transition metal nanosheets for biosensing applications. *Biosensors and Bioelectronics*, 2017, **89**(1), P. 201–211.

[11] Ruan S.B., Qian J., Shen S., Chen J.T., Zhu J.H., Jiang X.G., He Q., Yang W.L., Gao H.L. Fluorescent carbonaceous nanodots for noninvasive glioma imaging after angiopep-2 decoration. *Bioconjugate Chem.*, 2014, **25**, P. 2252–2259.

[12] Wang N., Zheng A.Q., Liu X., Chen J.J., Yang T., Chen M., Wang J.H. Deep eutectic solvent-assisted preparation of nitrogen/chloride-doped carbon dots for intracellular biological sensing and live cell imaging. *ACS Appl. Mater. Interfaces*, 2018, **10**, P. 7901–7909.

[13] Zholobak N.M., Shcherbakov A.B., Ivanova O.S., Reukov V., Baranchikov A.E., Ivanov V.K. Nanoceria-curcumin conjugate: synthesis and selective cytotoxicity against cancer cells under oxidative stress conditions. *J. Photochem. Photobiol. B.*, 2020, **209**, P. 111921.

[14] Shydlovska O., Kharchenko E., Zholobak N., Shcherbakov A., Marynin A., Ivanova O., Baranchikov A., Ivanov V. Cerium oxide nanoparticles increase cytotoxicity of TNF-alpha *in vitro*. *Nanosyst. Phys. Chem. Math.*, 2018, **9**(4), P. 537–543.

[15] Zholobak N.M., Shcherbakov A.B., Bogorad-Kobelska A.S., Ivanova O.S., Baranchikov A.Y., Spivak N.Y., Ivanov V.K. Panthenol-stabilized cerium dioxide nanoparticles for cosmeceutic formulations against ROS-induced and UV-induced damage. *J. Photochem. Photobiol. B.*, 2014, **130**, P. 102–108.

[16] Popova N.R., Shekunova T.O., Popov A.L., Selezneva I.I., Ivanov V.K. Cerium oxide nanoparticles provide radioprotective effects upon X-ray irradiation by modulation of gene expression. *Nanosyst. Phys. Chem. Math.*, 2019, **10**(5), P. 564–572.

[17] Fritsche E., Haarmann-Stemmann T., Kapr J., Galanjuk S., Hartmann J., Mertens P. R., Kämpfer A.A.M., Schins R.P.F., Tigges J., Koch K. Stem cells for next level toxicity testing in the 21st century. *Small*, 2021, **17**(15), P. 2006252.

[18] Zhang M., Bai L., Shang W., Xie W., Ma H., Fu Y., Fang D., Sun H., Fan L., Han M., Liu C., Yang S. Facile synthesis of water-soluble, highly fluorescent graphenequantum dots as a robust biological label for stem cells. *J. Mater. Chem.*, 2012, **22**, P. 7461–7467.

[19] Shao D., Lu M., Xu D., Zheng X., Pan Y., Song Y., Xu J., Li M., Zhang M., Li J., Chi G., Chen L., Yang B. Carbon dots for tracking and promoting the osteogenic differentiation of mesenchymal stem cells. *Biomater. Sci.*, 2017, **5**, P. 1820–1827.

[20] Brix N., Samaga D., Hennel R., Gehr K., Zitzelsberger H., Lauber, K. The clonogenic assay: robustness of plating efficiency-based analysis is strongly compromised by cellular cooperation. *Radiat. Oncol.*, 2020, **15**, P. 248.

[21] Brix N., Samaga D., Belka C., Zitzelsberger H., Lauber K. Analysis of clonogenic growth *in vitro*. *Nature protocols*, 2021, **16**, P. 4963–4991.

[22] Popov A., Abakumov M., Savintseva I., Ermakov A., Popova N., Ivanova O., Kolmanovich D., Baranchikov A., Ivanov V. Biocompatible dextran-coated gadolinium-doped cerium oxide nanoparticles as MRI contrast agents with high T1 relaxivity and selective cytotoxicity to cancer cells. *J. Mater. Chem. B*, 2021, **9**, P. 6586–6599.

[23] de Araújo Vieira L.F., Lins M.P., Nicácio Viana I.M.M., dos Santos J.E., Smaniotto S., dos Santos Reis M.D. Metallic nanoparticles reduce the migration of human fibroblasts *in vitro*. *Nanoscale res. lett.*, 2017, **12**(1), P. 200.

[24] Ribeiro F.M., de Oliveira M.M., Singh S., Sakthivel T.S., Neal C.J., Seal S., Ueda-Nakamura T., Lautenschlager S.O.S., Nakamura C.V. Ceria nanoparticles decrease UVA-induced fibroblast death through cell redox regulation leading to cell survival, migration and proliferation. *Front. Bioeng. Biotechnol.*, 2020, P. 1133.

[25] Xiao Y., Li J., Wang S., Yong X., Tang B., Jie M., Dong H., Yang X., Yang S. Cerium oxide nanoparticles inhibit the migration and proliferation of gastric cancer by increasing DHX15 expression. *Int J Nanomedicine*, 2016, **11**, P. 3023–3034.

[26] Chen D., Li B., Lei T., Na D., Nie M., Yang Y., Xie C., He Z., Wang J. Selective mediation of ovarian cancer SKOV3 cells death by pristine carbon quantum dots/Cu_2O composite through targeting matrix metalloproteinases, angiogenic cytokines and cytoskeleton. *J Nanobiotechnol*, 2021, **19**, P. 68.

[27] Manzanares D., Ceña V. Endocytosis: The nanoparticle and submicron nanocompounds gateway into the cell. *Pharmaceutics*, 2020, **12**, P. 371.

[28] Clément M. V., Ponton A., Pervaiz S. Apoptosis induced by hydrogen peroxide is mediated by decreased superoxide anion concentration and reduction of intracellular milieu. *FEBS letters*, 1998, **440**(1-2), P. 13–18.

[29] Clark A., Zhu A., Sun K., Petty H.R. Cerium oxide and platinum nanoparticles protect cells from oxidant-mediated apoptosis. *J Nanopart Res.*, 2011, **13**(10), P. 5547–5555.

[30] Pagliari F., Mandoli C., Forte G., Magnani E., Pagliari S., Nardone G., Licoccia S., Minieri M., Di Nardo P., Traversa E. Cerium oxide nanoparticles protect cardiac progenitor cells from oxidative stress. *ACS Nano*, 2012, **6**(5), P. 3767–3775.

[31] Weng Q., Sun H., Fang C., Xia F., Liao H., Lee H., Wang J., Xie A., Ren J., Guo X., Li F., Yang B., Ling D. Catalytic activity tunable ceria nanoparticles prevent chemotherapy-induced acute kidney injury without interference with chemotherapeutics. *Nat.Commun.*, 2021, **12**, P. 1436.

Submitted 8 February 2022; accepted 26 March 2022

Information about the authors:

A. L. Popov – Institute of Theoretical and Experimental Biophysics of the Russian Academy of Sciences, Institutskaya str., 3, Pushchino, 142290, Russia; antonpopovleonid@gmail.com

I. V. Savintseva – Institute of Theoretical and Experimental Biophysics of the Russian Academy of Sciences, Institutskaya str., 3, Pushchino, 142290, Russia; savintseva_irina@mail.ru

A. M. Ermakov – Institute of Theoretical and Experimental Biophysics of the Russian Academy of Sciences, Institutskaya str., 3, Pushchino, 142290, Russia; ao_ermakovy@rambler.ru

N. R. Popova – Institute of Theoretical and Experimental Biophysics of the Russian Academy of Sciences, Institutskaya str., 3, Pushchino, 142290, Russia; nellipopovaran@gmail.com

D. D. Kolmanovich – Institute of Theoretical and Experimental Biophysics of the Russian Academy of Sciences, Institutskaya str., 3, Pushchino, 142290, Russia; kdd100996@mail.ru

N. N. Chukavin – Institute of Theoretical and Experimental Biophysics of the Russian Academy of Sciences, Institutskaya str., 3, Pushchino, 142290, Russia; Moscow Region State University, 141014, Moscow, Russia; chukavinnik@gmail.com

A. F. Stolyarov – Institute of Theoretical and Experimental Biophysics of the Russian Academy of Sciences, Institutskaya str., 3, Pushchino, 142290, Russia; a.f.stolyaroff@gmail.com

A. B. Shcherbakov – Zabolotny Institute of Microbiology and Virology, National Academy of Sciences of Ukraine, Kyiv D0368, Ukraine; ceroform@gmail.com

O. S. Ivanova – Kurnakov Institute of General and Inorganic Chemistry of the Russian Academy of Sciences, Leninskiy prosp., 31, Moscow, 119991, Russia; runetta05@mail.ru

V. K. Ivanov – Kurnakov Institute of General and Inorganic Chemistry of the Russian Academy of Sciences, Leninskiy prosp., 31, Moscow, 119991, Russia; van@igic.ras.ru

Conflict of interest: the authors declare no conflict of interest.